Published in final edited form as:
J Am Chem Soc. 2010 January 13; 132(1): 106–111. doi:10.1021/ja908555n.

User-loaded SlipChip for equipment-free multiplexed nanoliter-scale experiments

Liang Li, **Wenbin Du**, and **Rustem Ismagilov***
Department of Chemistry and Institute for Biophysical Dynamics, The University of Chicago, 929 East 57th Street, Chicago, IL 60637

Abstract

This paper describes a microfluidic approach to perform multiplexed nanoliter-scale experiments by combining a sample with multiple different reagents, each at multiple mixing ratios. This approach employs a user-loaded, equipment-free SlipChip. The mixing ratios, characterized by diluting a fluorescent dye, could be controlled by the volume of each of the combined wells. The SlipChip design was validated on ~12 nL scale by screening the conditions for crystallization of glutaryl-CoA dehydrogenase from *Burkholderia pseudomallei* against 48 different reagents; each reagent was tested at 11 different mixing ratios, for a total of 528 crystallization trials. The total consumption of the protein sample was ~ 10 μL. Conditions for crystallization were successfully identified. The crystallization experiments were successfully scaled up in well plates using the conditions identified in the SlipChip. Crystals were characterized by X-ray diffraction and provided a protein structure in a different space group and at a higher resolution than the structure obtained by conventional methods. In this work, this user-loaded SlipChip has been shown to handle reliably fluids of diverse physicochemical properties, such as viscosities and surface tensions. Quantitative measurements of fluorescent intensities and high-resolution imaging were straighforward to perform in these glass SlipChips. Surface chemistry was controlled using fluorinated lubricating fluid, analogous to the fluorinated carrier fluid used in plug-based crystallization. Thus, we expect this approach to be valuable in a number of areas beyond protein crystallization, especially those areas where droplet-based microfluidic systems have demonstrated successes, including measurements of enzyme kinetics and blood coagulation, cell-based assays, and chemical reactions.

Introduction

This paper describes a SlipChip-based microfluidic approach for combining a sample with many different reagents, each at many different mixing ratios, to perform multiplexed nanoliter-scale experiments in a user-loaded, equipment-free fashion. Multiplexed experiments are common in the areas of biological assays,[1,2] chemical synthesis,[3,4] crystallization of proteins[5,6] and any area where chemical space is widely explored.[7,8] Wide exploration of chemical space benefits from technologies for faster experiments and lower consumption of samples, both to make these processes more productive and to reduce the amount of chemical waste.[9] Microfluidic technology has both the capacity for high throughput screening and the ability to manipulate fluids on nanoliter and smaller scales. Although various microfluidic systems have been developed for such applications,[10-16] these systems require pumps,[17] valves,[18] or centrifuges.[19] Recently, we reported the SlipChip,[20] which performs multiplexed microfluidic reactions without pumps or valves and whose operation requires only pipetting

r-ismagilov@uchicago.edu.

Supporting Information Available. Chemicals and materials, detailed experimental procedures, additional figures and tables, and two supporting movies. This material is available free of charge via the internet at http://pubs.acs.org. (PDF).

of a sample into the chip followed by slipping one part of the chip relative to another to combine the sample with pre-loaded reagents and initiate the reactions. Pre-loading the reagents onto the chips in a centralized facility and distributing chips to researchers is attractive to dramatically simplify the experiment for the user. Preloading may be problematic, however, for unstable reagents, or for experiments where reagents are custom-designed for each experiment. Here we report a SlipChip that does not have to be pre-loaded with reagents. It uses a principle similar to the one described in the previously developed SlipChip[20]: sliding of plates of a device relative to one another. Moving of parts of devices relative to one another is also used in devices that control fluid flow, including HPLC valves, microfluidic devices,[21-23] devices used to perform reactions,[24] and chromatography.[25,26] We show that this SlipChip can be used to perform multiplexed nanoscale experiments with many different reagents, each at multiple different mixing ratios, allowing exploration of chemical space on the regional scale. We validate this approach by screening conditions for crystallization of a soluble protein. Obtaining crystals of proteins remains one of the bottlenecks when solving their structures and elucidating their functions at the molecular level. Getting "diffraction-quality" crystals requires high throughput screening of multiple precipitants at various concentrations[27] –i.e. performing hundreds or thousands of crystallization trials. Microfluidic technology can use either valves[28] or droplets[17] to accurately handle nanoliter and even picoliter volumes, and has also been applied to crystallization of proteins.[18,29-31] Although these two approaches can successfully crystallize proteins, most individual laboratories are still setting up crystallization trials by pipetting microliters of solutions into 96-well plates, suggesting that there is still a need for a system for crystallizing proteins that is simple, inexpensive, fast, and controllable. Here we describe the development and validation of a user-loaded SlipChip that satisfies these criteria.

Results and Discussion

The general illustration of how a user-loaded SlipChip can be created is shown in Figure 1. In this paper, we designed the SlipChip to be able to screen a protein sample against 16 different precipitants, at 11 mixing ratios each, for a total of 176 experiments, each on the scale of ~12 nL, and requiring only 3.5 μL of the protein sample for all of the experiments (Figures 2 and 3). The SlipChip contained 16 separate fluidic paths for the reagents, each path with 11 wells, and a single, continuous fluidic path for the protein sample (Figure 2) with 176 wells. In some versions of this SlipChip, the inlets for fluidic paths of reagents were spaced in a way to match the spacing of wells in a 96-well plate and spacing of tips in a multichannel pipettor.

This SlipChip consisted of two plates. The top plate contained separate inlets for the reagent and the sample, ducts for the sample, and wells for the reagent (Figure 3A). The bottom plate contained ducts for the reagent which were connected to an inlet on the top plate, wells for the samples, and an outlet (Figure 3B). The two plates were separated by a layer of lubricating fluid,[20] for which we used fluorocarbon, a mixture of perfluoro–tri–n–butylamine and perfluoro–di–n–butylmethylamine (FC-40). When the two plates were first assembled (Figure 3C), the inlet and wells for the reagent in the top plate were aligned on top of the ducts for the reagent in the bottom plate. In this orientation, each reagent was pipetted into the inlet, flowed through the ducts, and filled the wells (Figure 3D). After loading the reagents, the top plate of the chip was "slipped" to a new orientation, where the ducts for the sample in the top plate were aligned on top of the wells for the sample in the bottom plate. In this orientation, the sample was pipetted into the inlet, flowed through the ducts, and filled the wells (Figure 3E). After loading both sample and reagents, the top plate of the chip was slipped again to position the wells for the reagent on top of the wells for the sample and initiating the interaction between the reagent and the sample taking place by diffusion (Figure 1F and 3F, see also supporting movie S1 and supporting movie S2. Supporting movie S1 was generated from images used to construct Figure 1, supporting movie S2 was generated from microphotographs of a SlipChip

with a related but not identical design to the one presented in Figure 3). We ensured that we addressed potential for cross-contamination during each of the slipping steps (e.g. between Figure 3D and Figure 3E). During the slipping steps a thin film of reagent solution can form between the two plates of the SlipChip. This thin film could connect the duct for the reagent to the well for the reagent instead of keeping them separated. Cross-contamination after the slipping steps was prevented by controlling the contact angle between the solutions (sample or reagents) and the plates of the SlipChip, measured under the lubricating fluid. We measured the contact angle under the lubricating fluid, fluorocarbon (FC), and determined that the contact angle must be above ~ 130° to prevent cross-contamination. To confirm this, when we loaded a solution of reagents containing no surfactants and having a contact angle of 139° (Table S1), the reagents did not get trapped between the plates of the SlipChip after the first slipping step. The contact angle requirement is the same for the second slipping step. To confirm this, when we added surfactant to the sample solution, the contact angle dropped to 110°, and a thin film of the surfactant solution was trapped between the two plates of the SlipChip. To eliminate this problem, we spin-coated the plates with thin layers of fluorinated ethylene propylene (FEP) and the contact angle increased to 154°. After spin coating, the slipping steps were performed without cross-contamination.

Using this SlipChip, we controlled the volumes, and thus the mixing ratio, of both the sample and reagents that were combined into each trial. We designed this SlipChip with wells for reagent and samples such that the total volume of a trial, created by slipping to combine the two wells, was always ~ 12 nL, and the mixing ratio of reagent and sample in each trial varied from 0.67:0.33 to 0.33:0.76 by volume, with nine evenly spaced ratios in between (Figure 4A).

Experimental results using a fluorescent dye solution as the sample and a buffer solution as the reagent confirmed that this design did lead to a controlled mixing ratio in each of the 11 wells. The relationship between the relative concentrations of the sample from the experiment and the predicted concentrations based on the design showed good agreement (Figure 4B, slope = 0.98; R^2 = .9938). Also, the disparity between the experimental and predicted concentrations was lower than 10% for all except for one of the wells (Figure 4C).

To test whether this approach would function reproducibly for a complex solution, we tested it with crystallization of a model membrane protein, the photosynthetic reaction center (RC) from *Blastochloris viridis*. Seven replicate trials, each with 11 different mixing ratios of a precipitant (3.2 M $(NH_4)_2SO_4$ in 40 mM NaH_2PO_4/Na_2HPO_4, pH 6.0) and RC, were performed on the SlipChip and were reproducible (Figure 5A). For this experiment, the different mixing ratios were randomly arranged across the rows of the SlipChip. That is, instead of beginning at a mixing ratio of 0.33 precipitant to 0.67 protein and ending at a mixing ratio of 0.67 precipitant to 0.33 protein with evenly spaced mixing ratios in between, the wells were arranged from left to right in the following order with regard to the relative precipitant concentration: 0.33, 0.63, 0.4, 0.57, 0.47, 0.5, 0.53, 0.43, 0.6, 0.37, and 0.67. This arrangement was chosen so that any artifacts of manufacturing or evaporation that might systematically skew the results from one side to another could be easily differentiated from the effects of mixing ratios. This arrangement also kept the distance between two adjacent wells similar, keeping the duct length similar as well, making fabrication of the SlipChip simpler. The results seen here were the same as when the different mixing ratios were arranged sequentially across the rows of the SlipChip in our previous experiments, indicating that any effects due to manufacturing or evaporation are minimal.

To help understand the behavior of crystallization, we digitally re-arranged the microphotographs of the wells in order of increasing concentration of the precipitant (Figure 5B). At mixing ratios of precipitant to protein from 0.33: 0.67 to 0.43:0.57, none of the seven trials formed protein crystals. At a mixing ratio of 0.47: 0.53, one trial formed protein crystals,

and at 1:1 four trials formed protein crystals. At mixing ratios of 0.53:0.47, 0.57:0.43 and 0.6:0.4, all seven trials formed protein crystals. At 0.63:0.37, all seven trials formed precipitate. At 0.67:0.33, two trials formed protein crystals while the remaining five formed precipitate. These results are consistent with the three expectations: 1) Crystallization of RC was sensitive to precipitant concentration. As we increased the relative concentration of precipitant, we observed a transition from the protein remaining in solution to crystallizing to precipitating (Figure 5B). 2) Decreasing protein concentration reduced nucleation to a certain extent, as we observed when transitioning from well sets 2 to 11 and from well sets 4 to 9 (Figure 5B). 3) Crystallization outcome was not monotonic with mixing ratio,[20] with regions of larger single crystals separated by regions of microcrystals. In addition to the seven rows used for the seven experiments described here, on this chip two rows were intentionally left blank and the additional seven trials were performed at a higher concentration of precipitant. These results were consistent with the results reported in Figure 5, but we did not present them here because as expected, they produced mostly precipitation and therefore were less diagnostic.

Finally, to validate this SlipChip design, we screened the conditions for crystallization of protein samples using many different reagents, each at many different mixing ratios, on a single user-loaded SlipChip. We chose a soluble protein as our target: glutaryl-CoA dehydrogenase from *Burkholderia pseudomallei*. The protein sample was obtained from the Seattle Structural Genomics Center for Infectious Disease (SSGCID). It was screened in parallel using SSGCID facilities to yield crystals under vapor diffusion conditions in conditions using 20% (w/v) PEG-3000, 0.1M HEPES pH 7.5, 0.2M NaCl (PDBid 3D6B). These crystals yielded a structure of 2.2 Å resolution and space group $P2_12_12_1$ (PDBid 3D6B). Without any knowledge of SSGCID crystallization conditions, we screened the protein against 48 different reagents from a home-made screening kit based on the Wizard screen (see Table S2). For each reagent, 11 different mixing ratios of protein sample and reagent were screened, ranging from 0.33:0.67 to 0.67:0.33 as described above. The screen successfully identified two conditions for crystallization of the protein, summarized in the Supporting Information (Table S3). From these results, optimal conditions were chosen: a 0.57:0.43 mixing ratio with 45% (w/v) PEG-400, 0.2 M $MgCl_2$ and 0.1 M Tris, pH 7.8 (Figure 6A) and a 0.67:0.33 mixing ratio with 30% (w/v) PEG-8000 and 0.1 M Hepes, pH 7.8 (Figure 6C). The latter condition is similar, but not identical, to the one identified by using traditional technologies at SSGCID. Each of these conditions was reproduced in well plates (see Supporting Information Experimental Procedures, Figure S3), and crystals were obtained in both cases (Figure 6B and D). The crystals from the well plates diffracted X-rays at resolutions of 1.6 Å (Figure 7A), space group $P2_1$ and 2.9 Å, space group $P2_12_12_1$ respectively (Table S4). Consequently, we determined the structure of the protein at the resolution of 1.73 Å (Figure 7B), with the data set collected from the crystal that diffracted X-rays to the higher resolution, 1.6 Å, and we could assign the loops missing in the 2.2 Å $P2_12_12_1$ structure. Interpretation of this structure is beyond the scope of this paper and will be discussed in a future publication; rather, this protein served as a case study illustrating that this approach can be used to identify new crystallization conditions, and that these conditions can be successfully scaled up using conventional crystallization techniques.

Conclusion

This paper described a user-loaded, equipment-free SlipChip that has been developed to perform multiplexed reactions by screening many different reagents against a substrate at different mixing ratios and accurately meter nanoliter volumes. This SlipChip could be also delivered to researchers preloaded with reagents at multiple mixing ratios or user-loaded at the site of use, depending on the requirements of a given application. The fluid paths were designed to include extra channels to increase fluidic resistance and to provide adequate filling of all wells. This method is functionally equivalent to the droplet-based hybrid method where many

different conditions are screened in a droplet-based array.[30,32] We have demonstrated the use of this SlipChip in screening conditions for crystallization for a soluble protein. X-ray diffraction data for the protein studied in this paper were obtained by replicating crystallization conditions in well plates, indicating that crystallization conditions identified in a SlipChip can be reliably scaled up outside of the SlipChip. The accompanying paper[33] describes crystallization by free interface diffusion on SlipChip and a composite SlipChip that performs both microbatch and free interface diffusion crystallizations in parallel.

Outside of crystallization, this user-loaded, equipment-free SlipChip should be applicable to a number of other multiplexed reactions and assays where both different reagents and their concentrations need to be tested. This SlipChip enables similar control of surface chemistry as in previously developed plug-based microfluidic systems because of the use of the fluorinated lubricating fluid.[34-36] Assays with enzymes,[37] blood,[38,39] and cells[32,34] have been performed in plug-based systems, so we expect that similar assays can be performed in SlipChip. We also expect this approach to be useful for analysis of samples obtained by the chemistrode.[40-43]

We found imaging SlipChips to be more straightforward than imaging droplets, as positions of all wells are defined and curvature of the fluid-fluid interface is not a problem. We will be expanding the application of the user-loaded, equipment-free SlipChip for those applications where the droplet-based approaches,[12,37,38,44-48] especially the hybrid approach[30,32] have already been demonstrated. In general, attractive applications of user-loaded SlipChips span areas of diagnostics, drug discovery, combinatory chemistry, biochemistry, molecular biology and materials science.

Supplementary Material

Refer to Web version on PubMed Central for supplementary material.

Acknowledgments

This work was supported in part by NIH Roadmap for Medical Research R01 GM075827, by the NIH Protein Structure Initiative Specialized Centers Grant U54 GM074961 (ATCG3D), and by the NIH Director's Pioneer Award (1DP1OD003584). Use of the Argonne National Laboratory GM/CA beamlines at the Advanced Photon Source was supported by the U.S. Department of Energy, Basic Energy Sciences, Office of Science, under Contract No. DE-AC02-06CH11357. GM/CA CAT has been funded in whole or in part with Federal funds from the National Cancer Institute (Y1-CO-1020) and the National Institute of General Medical Science (Y1-GM-1104) We thank Kevin Nichols for providing the movie S1, frames of which were used to create Figure 1, James Norris of the University of Chicago for the generous gift of RC, and SSGCID for the samples of glutaryl-CoA dehydrogenase. SSGCID is supported by Federal Contract No.: HHSN272200700057C from NIAID to the Seattle Biomedical Research Institute and its collaborating subcontractors. We thank Elizabeth B. Haney and Heidi Park for contributions to writing and editing this manuscript. We thank Bart Staker for buddy-checking the structure of *glutaryl-CoA dehydrogenase* for PDB deposition.

References

1. Markoulatos P, Siafakas N, Moncany M. J. Clin. Lab. Anal 2002;16:47–51. [PubMed: 11835531]
2. Sharma RK, Rogojina AT, Chalam KV. Mol. Vis 2009;15:60–69. [PubMed: 19145248]
3. Lam KS, Lebl M, Krchnak V. Chem. Rev 1997;97:411–448. [PubMed: 11848877]
4. Uttamchandani M, Walsh DP, Yao SQ, Chang YT. Curr. Opin. Chem. Biol 2005;9:4–13. [PubMed: 15701446]
5. Durbin SD, Feher G. Annu. Rev. Phys. Chem 1996;47:171–204. [PubMed: 8983237]
6. McPherson, A. Crystallization of Biological Macromolecules. Cold Spring Harbor Laboratory Press; 1999.
7. de Vegvar HEN, Robinson WH. Clin. Immunol 2004;111:196–201. [PubMed: 15137952]
8. Epstein JR, Biran I, Walt DR. Anal. Chim. Acta 2002;469:3–36.

9. Persidis A. Nat. Biotechnol 1998;16:488–489. [PubMed: 9592401]
10. Squires TM, Quake SR. Rev. Mod. Phys 2005;77:977–1026.
11. Beebe DJ, Mensing GA, Walker GM. Annu. Rev. Biomed. Eng 2002;4:261–286. [PubMed: 12117759]
12. Dittrich PS, Manz A. Nat. Rev. Drug Discov 2006;5:210–218. [PubMed: 16518374]
13. Song H, Chen DL, Ismagilov RF. Angew. Chem.-Int. Edit 2006;45:7336–7356.
14. Whitesides GM. Nature 2006;442:368–373. [PubMed: 16871203]
15. Hansen C, Quake SR. Curr. Opin. Struct. Biol 2003;13:538–544. [PubMed: 14568607]
16. Jahnisch K, Hessel V, Lowe H, Baerns M. Angew. Chem.-Int. Edit 2004;43:406–446.
17. Song H, Tice JD, Ismagilov RF. Angew. Chem.-Int. Edit 2003;42:768–772.
18. Hansen CL, Skordalakes E, Berger JM, Quake SR. Proc. Natl. Acad. Sci. U. S. A 2002;99:16531–16536. [PubMed: 12486223]
19. Madou M, Zoval J, Jia GY, Kido H, Kim J, Kim N. Annu. Rev. Biomed. Eng 2006;8:601–628. [PubMed: 16834568]
20. Du WB, Li L, Nichols KP, Ismagilov RF. Lab Chip 2009;9:2286–2292. [PubMed: 19636458]
21. Yin NF, Killeen K, Brennen R, Sobek D, Werlich M, van de Goor TV. Anal. Chem 2005;77:527–533. [PubMed: 15649049]
22. Kuwata, M.; Kitamori, T. microTAS. Tokyo, Japan: 2006. p. 1130-1132.
23. Tokeshi, M.; Kitamori, T. Advances in Flow Analysis. Trojanowicz, M., editor. Wiley-VCH; 2008. p. 149-166.
24. Moerman R, van Dedem GWK. Anal. Chem 2003;75:4132–4138. [PubMed: 14632126]
25. Desmet G, Baron GV. Anal. Chem 2000;72:2160–2165. [PubMed: 10815980]
26. Cai Y, Janasek D, West J, Franzke J, Manz A. Lab Chip 2008;8:1784–1786. [PubMed: 18941675]
27. Chayen NE, Saridakis E. Nat. Methods 2008;5:147–153. [PubMed: 18235435]
28. Unger MA, Chou HP, Thorsen T, Scherer A, Quake SR. Science 2000;288:113–116. [PubMed: 10753110]
29. Zheng B, Roach LS, Ismagilov RF. J. Am. Chem. Soc 2003;125:11170–11171. [PubMed: 16220918]
30. Li L, Mustafi D, Fu Q, Tereshko V, Chen DLL, Tice JD, Ismagilov RF. Proc. Natl. Acad. Sci. U. S. A 2006;103:19243–19248. [PubMed: 17159147]
31. Lau BTC, Baitz CA, Dong XP, Hansen CL. J. Am. Chem. Soc 2007;129:454–455. [PubMed: 17226984]
32. Boedicker JQ, Li L, Kline TR, Ismagilov RF. Lab Chip 2008;8:1265–1272. [PubMed: 18651067]
33. Li L, Du WB, Ismagilov RF. J. Am. Chem. Soc. 2009 (DOI: 10.1021/ja908558m).
34. Holtze C, Rowat AC, Agresti JJ, Hutchison JB, Angile FE, Schmitz CHJ, Koster S, Duan H, Humphry KJ, Scanga RA, Johnson JS, Pisignano D, Weitz DA. Lab Chip 2008;8:1632–1639. [PubMed: 18813384]
35. Kreutz JE, Li L, Roach LS, Hatakeyama T, Ismagilov RF. J. Amer. Chem. Soc 2009;131:6042–6043. [PubMed: 19354215]
36. Roach LS, Song H, Ismagilov RF. Anal. Chem 2005;77:785–796. [PubMed: 15679345]
37. Li L, Boedicker JQ, Ismagilov RF. Anal. Chem 2007;79:2756–2761. [PubMed: 17338503]
38. Song H, Li HW, Munson MS, Van Ha TG, Ismagilov RF. Anal. Chem 2006;78:4839–4849. [PubMed: 16841902]
39. Pompano RR, Li HW, Ismagilov RF. Biophys. J 2008;95:1531–1543. [PubMed: 18424502]
40. Chen D, Du WB, Liu Y, Liu WS, Kuznetsov A, Mendez FE, Philipson LH, Ismagilov RF. Proc. Natl. Acad. Sci. U. S. A 2008;105:16843–16848. [PubMed: 18974218]
41. Liu Y, Ismagilov RF. Langmuir 2009;25:2854–2859. [PubMed: 19239191]
42. Chen DL, Du W, Ismagilov R. New J. Phys 2009;11:075017.
43. Zheng B, Ismagilov RF. Angew. Chem.-Int. Edit 2005;44:2520–2523.
44. Chen DL, Gerdts CJ, Ismagilov RF. J. Am. Chem. Soc 2005;127:9672–9673. [PubMed: 15998056]
45. Beer NR, Hindson BJ, Wheeler EK, Hall SB, Rose KA, Kennedy IM, Colston BW. Anal. Chem 2007;79:8471–8475. [PubMed: 17929880]

46. Clausell-Tormos J, Lieber D, Baret JC, El-Harrak A, Miller OJ, Frenz L, Blouwolff J, Humphry KJ, Koster S, Duan H, Holtze C, Weitz DA, Griffiths AD, Merten CA. Chem. Biol 2008;15:427–437. [PubMed: 18482695]

47. deMello AJ. Nature 2006;442:394–402. [PubMed: 16871207]

48. Teh SY, Lin R, Hung LH, Lee AP. Lab Chip 2008;8:198–220. [PubMed: 18231657]

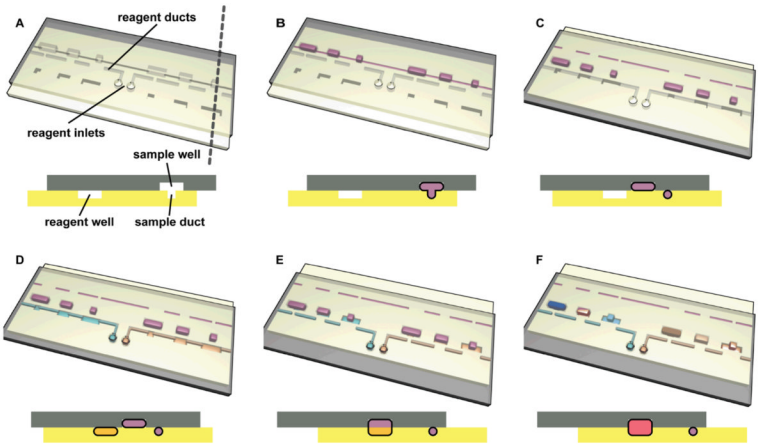

Figure 1.

Step-by-step 3D schematic drawings with cross-sectional views that describe the operation of a user-loaded SlipChip. (A) In the starting orientation, the two plates of the SlipChip are aligned such that the sample wells and sample ducts are aligned to form a continuous fluidic path, and the reagent wells and reagent ducts are offset. (B) The sample (purple) is loaded through the continuous fluidic path formed by overlapping sample wells (top plate) with sample ducts (bottom plate). (C) The device is slipped such that the reagent wells (bottom plate) and reagent ducts (top plate) are now aligned. (D) Reagents (blue and yellow) are loaded into the individual fluidic paths formed by overlapping reagent wells and sample wells. (E) The device is slipped a second time, and the sample wells from the top plate are exposed to the reagent wells of the bottom plate. (F) The pink well schematically shows a reaction taking place after mixing and incubation (see movie S1).

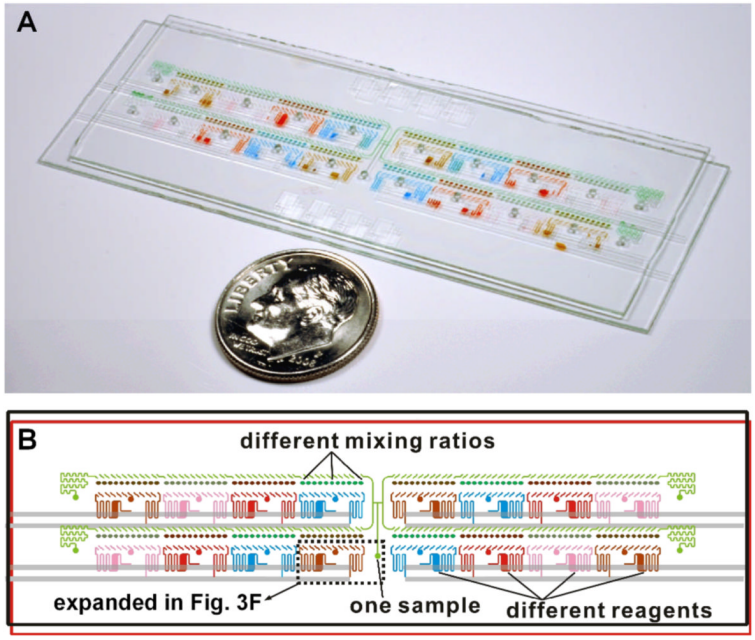

Figure 2.

A user- loaded SlipChip to screen one sample (green) against 16 different reagents (shown with other colors) at different concentrations. (A) A photograph of the SlipChip fabricated in glass with fluid paths filled with food dyes (US dime is shown for scale). (B) A schematic of the layout of the user-loaded SlipChip, expanded and operation explained in Figure 3.

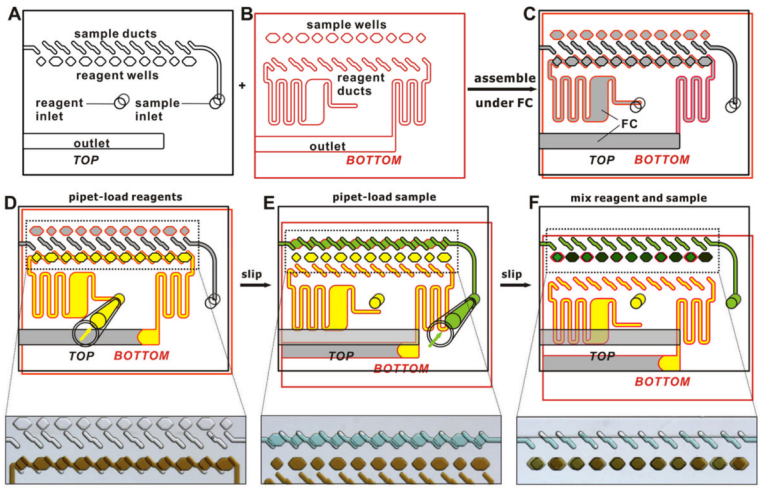

Figure 3.

A zoomed-in schematic of the area outlined in Figure 2B and corresponding experimental microphotographs showing the operation of the user-loaded SlipChip (see supporting movie S1). (A) The top plate (contoured in black) consisted of an outlet channel, a reagent inlet, a sample inlet aligned to sample ducts, and reagent wells. (B) The bottom plate (contoured in red) consisted of an outlet aligned with reagent ducts and sample wells. (C) The top plate and bottom plate were assembled and filled with fluorocarbon to generate a SlipChip ready for use. In this orientation, a continuous fluidic path was formed by the reagent inlet, the reagent wells, and the outlet. (D) A reagent was introduced by pipetting. The reagent (yellow) flowed through the continuous fluidic path and filled the reagent wells. A microphotograph below the schematic shows brown dye solution being loaded as the reagent. (E) The chip was slipped into a second position. In this second position, a continuous fluidic path was formed by the sample inlet, the sample ducts, and the sample wells. The sample (green) was introduced by pipetting. The sample flowed through the continuous fluidic path and filled the sample wells. A microphotograph below the schematic shows green dye solution being loaded as the sample. (F) The chip was slipped again into the third position, where the reagent wells were aligned on top of the sample wells, and the sample and reagent in the aligned wells combined by diffusion (dark green). A microphotograph below the schematic shows the reagent combining with the sample in each well, forming individual experiments. The colors of the reagent and the sample in D-F are not consistent for the schematics and the microphotographs. The colors in the schematic were changed to better illustrate the operation of the SlipChip.

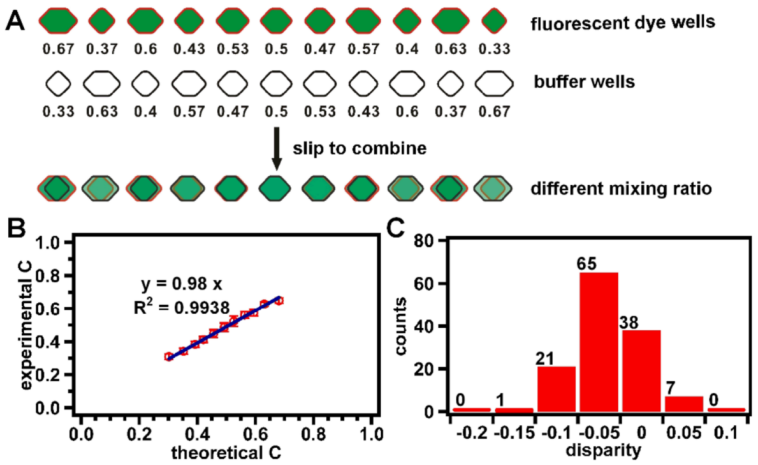

Figure 4.

Quantifying mixing ratios of reagents and sample in a SlipChip from Figures 2 and 3. A) A schematic of the experimental setup. This SlipChip had wells for the sample in the bottom plate (outlined in red) containing a fluorescent dye solution (green) and wells for the reagent in the top plate (outlined in black) containing a buffer solution (white). Each well was a different size and held a different volume of fluid, and the number under each well indicates the relative volume of the well. Wells ranged in volume from 8 nL (relative volume of 0.67) to 4 nL (relative volume of 0.33). Once the chip was slipped to combine the reagents and the sample, the total volume of a trial was always 12 nL. B) A graph of the relative concentrations of the diluted sample from the experiment (experimental C) plotted against the relative concentrations that were predicted based on the designed volume (theoretical C) shows a good agreement between the experimental and predicted concentrations (slope = 0.98; R^2 = 0.9938). The concentration was inferred from the measurements of fluorescent intensities. C) A histogram of the number of wells with different disparity values. The disparity was calculated as the percentage difference in concentration between the experiment results and the predicted concentration, and takes into account errors and deviations in fabrication of the wells, filling of the wells, slipping, and measurements of intensity.

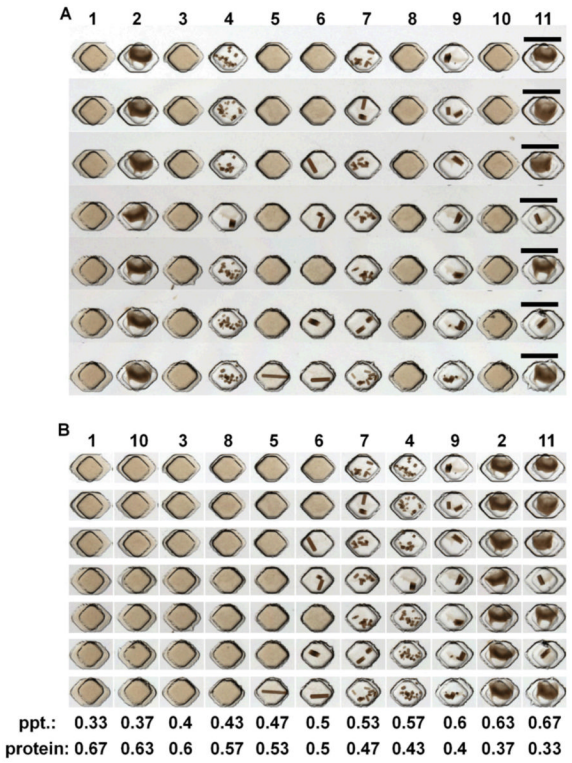

Figure 5.

Operation of the user-loaded SlipChip is reproducible, as illustrated by crystallization of the photosynthetic reaction center from *Blastochloris viridis*. (A) 11 trials using the same precipitant at different concentration ratios, each replicated seven times. Each row shows a replicate of each of the 11 concentration ratios, and each column shows all the replicates at a single concentration ratio. The ratios were randomized across the rows on the chip. The images were obtained after incubating for five days in the dark at room temperature. (B) The microphotographs of the wells in A were digitally re-arranged in order of increasing relative volume of reagent (precipitant, ppt) and decreasing volume of sample (protein) indicated under each column. Scale bars are 500 μm.

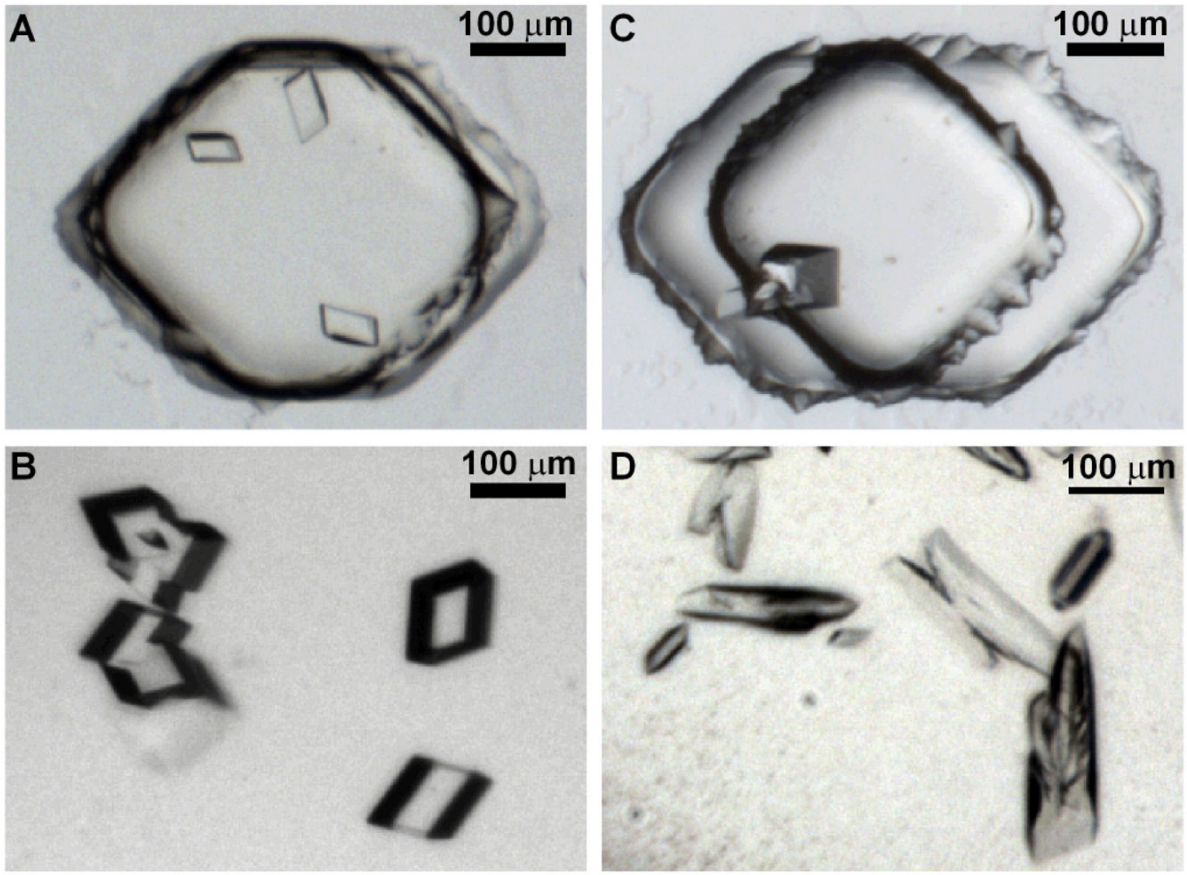

Figure 6.
Glutaryl-CoA dehydrogenase from *Burkholderia pseudomallei* was screened in user-loaded SlipChips against 48 different reagents, each at 11 different mixing ratios. (A) A microphotograph of crystals of glutaryl-CoA dehydrogenase in the SlipChip formed at a mixing ratio of 0.57:0.43 with 45% (w/v) PEG-400, 0.2 M $MgCl_2$ and 0.1 M Tris, pH 7.8. (B) A microphotograph of crystals of Glutaryl-CoA dehydrogenase reproduced by using the same mixing ratio as in (A) in well plates. (C) A microphotograph of crystals of glutaryl-CoA dehydrogenase in the SlipChip formed at a mixing ratio of 0.67:0.33 with 30% (w/v) PEG-8000 and 0.1 M Hepes, pH 7.5. (D) A microphotograph of crystals of glutaryl-CoA dehydrogenase reproduced by using the same mixing ratio as in (C) in well plates.

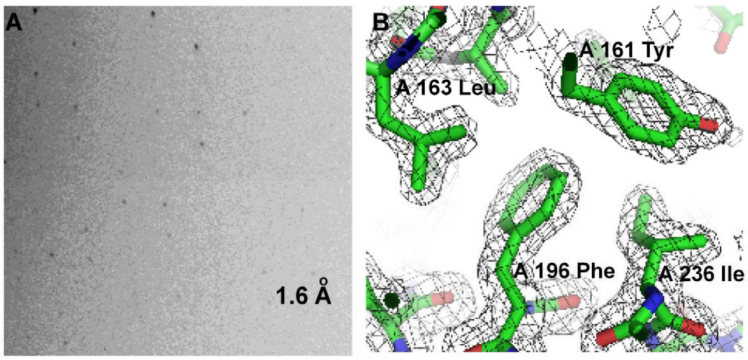

Figure 7.

Determination of the crystal structure of glutaryl-CoA dehydrogenase (PDBid 3II9). (A) An X-ray diffraction pattern obtained from crystals of glutaryl-CoA dehydrogenase (shown in Figure 6B) at a region of 1.6 Å resolution; (B) 2Fo-Fc Electron density map (grey) contoured at 1.2σ and refined model of glutaryl-CoA dehydrogenase derived from 1.73 Å resolution data. Residues 161 Tyr, 163 Leu, 196 Phe and 236 Ile from chain A display well-defined density.